Raman Spectra of High-Density, Low-Density, and Linear Low-Density Polyethylene Pellets and Prediction of Their Physical Properties by Multivariate Data Analysis

Harumi Sato,[1] Masahiko Shimoyama,[1,2] Taeko Kamiya,[1] Toru Amari,[3] Slobodan Šašic,[1] Toshio Ninomiya,[2] Heinz W. Siesler,[4] Yukihiro Ozaki[1]

[1]*School of Science, Kwansei-Gakuin University, Nishinomiya 662-8501, Japan*
[2]*Forensic Science Laboratory, Hyogo Prefectural Police Headquarters, Shimoyamate-dori, Chuo-ku, Kobe 650-8510, Japan*
[3]*Center for Analytical Chemistry and Sciences, Yokkaichi 510-1848, Japan*
[4]*Department of Physical Chemistry, University of Essen, Essen D-45117, Germany*

Received 27 August 2001; accepted 26 December 2001

ABSTRACT: Raman spectra have been measured for pellets of five samples of high-density polyethylene (HDPE), seven samples of low-density polyethylene (LDPE), and six samples of linear low-density polyethylene (LLDPE). The obtained Raman spectra have been compared to find out characteristic Raman bands of HDPE, LDPE, and LLDPE. Principal component analysis (PCA) was applied to the Raman spectra in the 1600–650 cm^{-1} region after multiplicative scatter correction (MSC) to discriminate the Raman spectra of the three different PE species. They are classified into three groups by a score plot of PCA factor 1 vs. 2. HDPE with high density and high crystallinity gives high scores on the factor 1 axis, while LDPE with low density and low crystallinity yields negative scores on the same axis. It seems that factor 1 reflects the density or crystallinity. A PC weight loadings plot for factor 1 shows six upward peaks corresponding to the bands arising from the crystalline parts or *all-trans* —$(CH_2)_n$— groups and seven downward peaks ascribed to the bands of the amorphous or anisotropic regions and those arising from the short branches. Partial least-squares (PLS-1) regression was applied to the Raman spectra after MSC to propose calibration models that predict the density, crystallinity, and melting points of the polyethylenes. The correlation coefficient was calculated to be 0.9941, 0.9800, and 0.9709 for the density, crystallinity, and melting point, respectively, and their root-mean-square error of cross validation (RMSECV) was found to be 0.0015, 3.3707, and 2.3745, respectively. The loadings plot of factor 2 for the prediction of melting point is largely different from those for the prediction of density and crystallinity. J Appl Polym Sci 86: 443–448, 2002

Key words: polyethylene; Raman spectroscopy; principal component analysis (PCA); partial least-squares (PLS) regression

INTRODUCTION

The first applications of Raman spectroscopy for the analysis of polymers date back nearly 40 years.[1–8] In the past, it was used mainly for qualitative analysis and conformational and orientational investigations. Quantitative analysis of polymers by Raman spectroscopy was not popular, although there were some pioneering studies.[1,6–8] It was also often difficult to obtain high-quality Raman spectra from polymers of practical importance because the interference of fluorescence was very severe. Raman spectroscopic studies of real-world polymers were rather limited, but this situation has changed partly due to the development of Raman instruments such as multichannel Raman spectrometers with a CCD detector and FT-Raman systems and partly because of the introduction of various spectral analysis methods such as two-dimensional (2D) correlation spectroscopy[9–11] and chemometrics.[12–14]

Recent progress in hardware and software of Raman spectroscopy has enabled one to use Raman spectroscopy as a powerful tool for quantitative analysis and process analysis of polymers.[8,15–29] Thanks to the development of multichannel Raman spectroscopy, one can obtain a number of high-quality Raman spectra of polymers in relatively short time. These Raman data are very suitable for various multivariate analysis approaches such as principal component analysis (PCA), partial least squares (PLS) regression, and self-modeling curve resolution (SMCR) methods.

We have been involved in Raman-chemometrics studies of polymers of practical importance to develop reliable calibration models predicting their physical and chemical properties on the one hand,[24–26] and on the other hand in Raman-SMCR investigations of polymers to explore the potential of SMCR methods in process analysis.[27–29] In our previous studies we pro-

Correspondence to: Y. Ozaki (ozaki@kwansei.ac.jp).

Journal of Applied Polymer Science, Vol. 86, 443–448 (2002)

posed a calibration model that predicts vinyl acetate contents in poly (ethylene vinyl acetate) copolymers by use of a combined Raman-PLS regression method.[24] We also developed a calibration model that predicts the density of linear low-density polyethylene (LLDPE) by the same method.[25] The purpose of our studies is not only to develop the calibration models but also to deepen the understanding of the spectral analysis of these polymers.

The aim of the present study is twofold. The one is to investigate the Raman spectra of high-density PE (HDPE), low-density PE (LDPE), and LLDPE in some detail. Raman spectra of PE have been extensively studied,[30–34] but a detailed comparison of Raman spectra of the three kinds of PEs has never been reported to the best of our knowledge. Another purpose of the present study is to develop calibration models that predict density, crystallinity, and melting point of PEs. These two purposes are closely related to each other. For example, loadings plots for the models predicting the physical properties play important roles in resolution enhancement of Raman bands.

The present study has the following novelty compared with the previous study on LLDPE by our group.[25]

1. The present study involves HDPE, LDPE, and LLDPE while the previous study investigated only LLDPE. The involvement of the three kinds of PE is very important to investigate (a) the differences in their Raman spectra, (b) the possibility of their classification by chemometrics, and (c) the calibration for wider ranges of densities and other physical properties.
2. The present study develops the calibration for the density, crystallinity, and melting point, whereas the previous one built the calibration only for the density.
3. The present study uses visible excitation with a Raman instrument equipped with a CCD detector. Thus, we can obtain Raman spectra of PEs much faster with much weaker laser power compared with the previous work that employed an FT-Raman system.

TABLE I
Density, Crystallinity, and Melting Points of 18 Samples of Polyethylene Pellet Used in the Present Study

Samples	Density (g/cm^3)	Crystallinity (%)	Melting points (°C)
HDPE (High-density polyethylene)			
HD1	0.952	68.3	128.4
HD2	0.951	63.7	129.8
HD3	0.958	70.4	130.0
HD4	0.964	74.7	132.4
HD5	0.960	66.6	132.5
LDPE (Low-density polyethylene)			
LD1	0.923	33.1	111.0
LD2	0.926	35.6	112.8
LD3	0.919	27.8	107.4
LD4	0.919	29.8	106.6
LD5	0.921	31.0	107.6
LD6	0.919	26.8	105.7
LD7	0.918	26.1	106.1
LLDPE (Linear low-density polyethylene)			
LL1	0.921	31.2	123.2
LL2	0.923	31.0	124.0
LL3	0.925	32.0	123.9
LL4	0.928	37.7	124.3
LL5	0.935	42.7	126.4
LL6	0.937	52.2	127.5

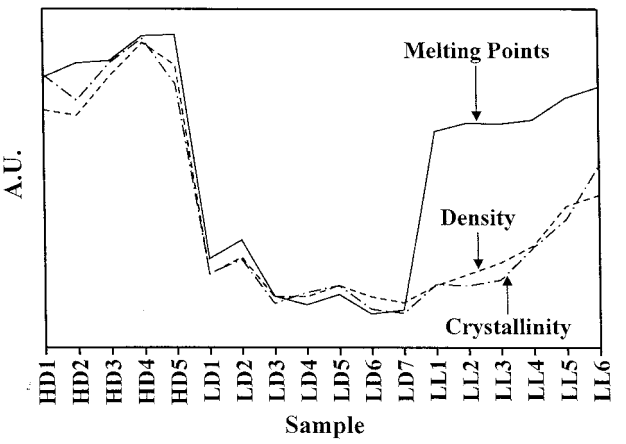

Figure 1 Comparison of the density, crystallinity, and melting point values of the investigated 18 different PEs.

The above three points are all very important from the points of applied polymer science.

EXPERIMENTAL

Samples

Five samples of HDPE, seven samples of LDPE, and six samples of LLDPE were obtained as pellets from Mitsubishi Chemical Co., and used as received. Table I summarizes their density, crystallinity, and melting points. Figure 1 compares the three physical properties of the 18 samples. The samples of LDPE and LLDPE have short branches such as ethyl and isobutyl groups that control their density. The density of the samples was determined by the density-gradient-tube method, whereas crystallinity and melting point of the samples were determined from DSC measurements.

Instruments

The Raman spectra of the polymer pellets (approx. 4 mm in diameter) were measured at a 4 cm^{-1} spectral resolution with a JASCO NRS 2001 Raman spectrometer equipped with a liquid-cooled CCD detector (LN/CCD-1100PBUVAR. Princeton Instruments). The

wave number calibration was performed by measuring a Raman spectrum of indene. The 514.5-nm line from an Ar laser (Spectra-Physics 2016) was used as an excitation source for the Raman spectra. The laser power at the sample position was typically 50 mW. Raman scattered light was collected with a 90° scattering geometry, and for each measurement, the exposure time and accumulation time were 10 s and 2 times, respectively.

Data analysis

For each sample three Raman spectra were recorded (54 spectra in total), and an average spectrum was calculated. The resulting 18 spectra were used for multivariate analysis. The Unscrambler (Version 6.2) software program (CAMO AS, Trondheim, Norway) was employed for spectral data analysis. The spectra in the 1600–650 cm^{-1} region after the treatment of multiplicative scatter correction (MSC) were subjected to the multivariate data analysis. The MSC treatment is very important for the multivariate data analysis of Raman spectral data because the absolute intensities of Raman bands change slightly for each measurement.[24–26]

The number of data points for each Raman spectrum was 1120. PCA was applied to the spectral data to discriminate the 18 kinds of the PE pellet samples while PLS-1 regression was used to develop calibration models that predict the density, crystallinity, and melting points of the 18 samples of PEs. In the PLS regression analysis, leave-one-out crossvalidation was performed for the 18 spectra to validate the models.

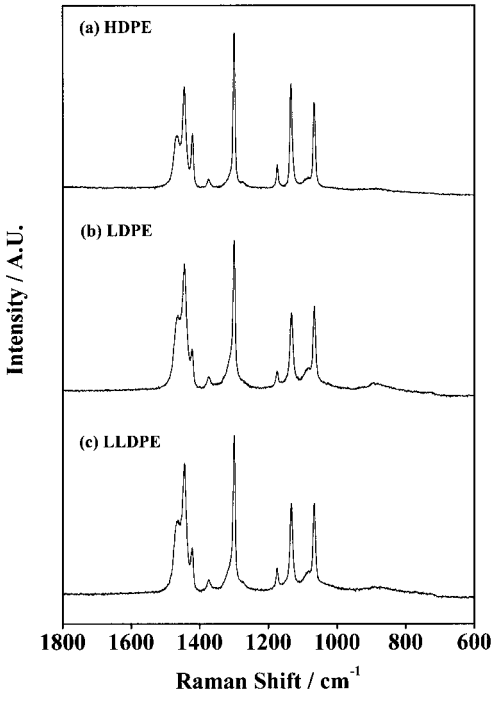

Figure 2 Representative Raman spectra of HDPE (a), LDPE (b), and LLDPE (c).

TABLE II
Band Assignments of Raman Bands of HDPE, LDPE, and LLDPE

Bands (cm^{-1})	Assignments	Features[a]
1465	2 × CH_2 rocking	C, N
1454	CH_2 bending	N
1445	CH_2 bending	C
1434	CH_2 bending	N
1421	CH_2 bending	C
1374	CH_2 wagging	A
1308	CH_2 twisting	A
1299	CH_2 twisting	C, N
1174	CH_2 rocking	C
1132	C—C stretching	C, N
1084	C—C stretching	A
1067	C—C stretching	C, N
897	C—C stretching (branches)	A

[a] A: amorphous; C: crystalline; N: anisotropic.

RESULTS AND DISCUSSION

Comparison of Raman spectra of HDPE, LDPE, and LLDPE

Figure 2 shows the Raman spectra of representative HDPE (a), LDPE (b), and LLDPE (c) pellet samples, respectively. Raman spectra of PEs have been studied very well.[30–34] Table II summarizes the assignments of Raman bands of HDPE, LDPE, and LLDPE. The assignments are based upon previous studies of the Raman spectra of various PEs, comparison of Raman spectra of HDPE, LDPE, and LLDPE, loadings plots of PCA factor 1 and 2 for the 18 samples of investigated PEs, and PLS loadings plots for models predicting the density, crystallinity, and melting point.

Comparison of the Raman spectra of the three kinds of PEs allows us to discuss characteristics of Raman spectra of HDPE, LDPE, and LLDPE. The Raman spectrum of LDPE shows an unresolved feature near 1454 cm^{-1} due to anisotropic parts, broad features near 1308 and 1084 cm^{-1} attributed to amorphous parts, and broad bands at 897 and 815 cm^{-1} characteristic of the short branches. The Raman spectrum of HDPE is characterized by sharp and intense bands at 1445 and 1421 cm^{-1} due to the correlation splitting of the CH_2 bending vibrations of the crystalline regions. Bands at 1299, 1132, and 1067 cm^{-1} arising from *all-trans* —$(CH_2)_n$— groups are also sharp and strong in the Raman spectrum of HDPE. The Raman spectrum of LLDPE shows spectral features in between the Raman spectra of HDPE and LDPE.

Discrimination of Raman spectra of HDPE, LDPE, and LLDPE by PCA

Figure 3 shows a score plot of PCA factor 1 vs. factor 2 for the five samples of HDPE, the seven samples of

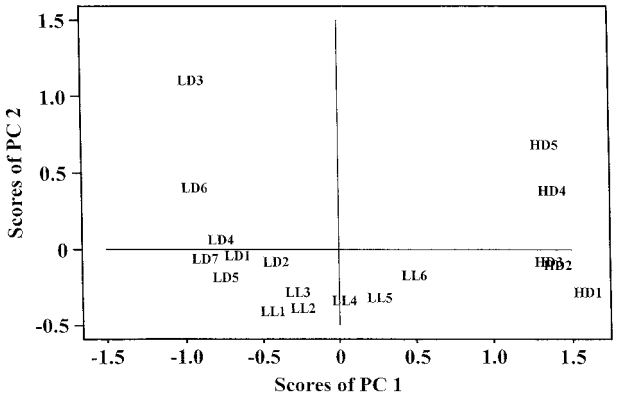

Figure 3 Score plot of PCA factor 1 vs. factor 2 for the 18 samples of HDPE, LDPE, and LLDPE based on their 18 Raman spectra in the 1600–650 cm^{-1} region.

LDPE, and the six different LLDPEs based on their 18 Raman spectra. Factor 1 and factor 2 explain 80 and 13% of variance, respectively. Note that the three kinds of PEs are clearly discriminated by PCA. It can be seen from Figure 3 that the score on factor 1 reflects the density and crystallinity of the PEs. HDPE that shows high density and high crystallinity yields high score values on the factor 1 axis while LDPE that shows low density and low crystallinity yields negative score values on the same axis. Within each group of the different species there is also a clear tendency

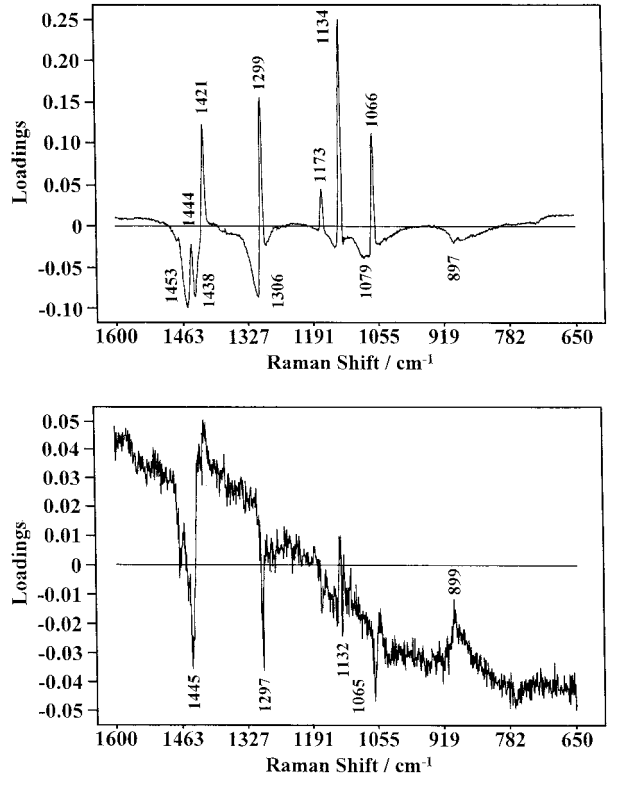

Figure 4 PCA loadings plot of factor 1 (A) and factor 2 (B) for the model shown in Figure 3.

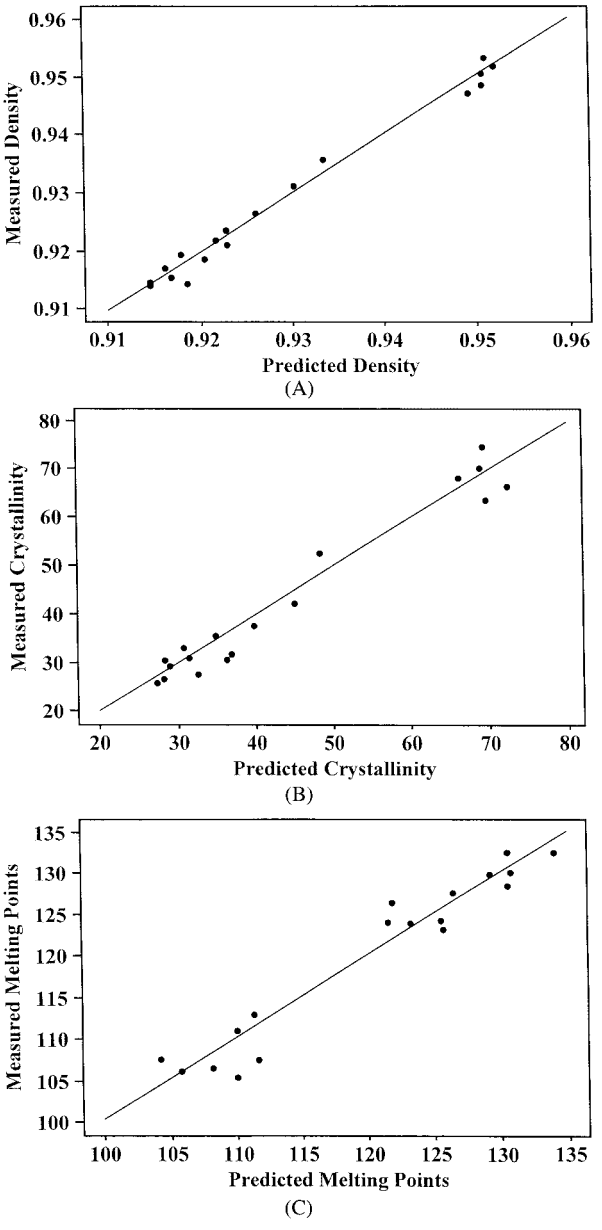

Figure 5 PLS regression calibration models for the prediction of the density (A), crystallinity (B), and melting point (C) of HDPE, LDPE, and LLDPE from the Raman spectra in the 1600–650 cm^{-1} region.

that the higher the density or crystallinity, the higher the score value on factor 1. For example, the order of density in the six samples of LLDPE is LL6, LL5, LL4, LL3, LL2, and LL1, and the order of the score values on factor 1 is LL6, LL5, LL4, LL2, LL3, and LL1. In contrast to factor 1, it is rather difficult to interpret the variation of the score values of factor 2.

Figure 4(A) and (B) displays the PC loadings plots of factor 1 and factor 2, respectively. A PC weight loadings plot of factor 1 [Fig. 4(A)] shows six sharp upward peaks at 1444, 1421, 1299, 1173, 1134, and 1066 cm^{-1} and seven rather broad downward features at 1453, 1438, 1306, 1079, 897, and 815 cm^{-1}. All the

TABLE III
Selected Parameters of the PLS Models for the Prediction of Density, Crystallinity, and Melting Point

Property	Correlation	RMSECV	Factor
Density	0.9941	0.0015	2
Crystallinity	0.9800	3.3707	2
Melting point	0.9709	2.3745	4

upward peaks correspond to the bands arising from the crystalline parts or *all-trans* —$(CH_2)_n$— groups (Table II). On the other hand, the downward peaks above 1000 cm^{-1} can be attributed to the bands due to amorphous or anisotropic regions and downward peaks at 897 and 815 cm^{-1} correspond to the bands assignable to the short branches. Therefore, the PC weight loadings plot reveals that factor 1 reflects variations in the crystallinity. The crystallinity is directly related to the density of the corresponding sample. Thus, factor 1 reflects also variations in the density.

Particularly noted in Figure 4(A) is that bands that are not clearly detected in the original spectra appear in the PC weight loadings plot. For example, the peaks at 1453, 1438, and 1306 cm^{-1} in the loadings plot cannot be found in the original spectra as a separate band. Therefore, in other words, the loadings plot has a deconvolution ability for overlapped bands.

The PC weight loadings plot of factor 2 [Fig. 4(B)] is quite different from that of factor 1. It is not easy to interpret the plot of factor 2, but it is noted that most of the peaks are assignable to the bands arising from the crystalline or anisotropic regions.

Prediction of the density, crystallinity, and melting point of PEs by PLS regression

Figure 5(A), (B), and (C) shows PLS-1 regression calibration models that predict the density, crystallinity, and melting point of the investigated PEs, respectively. Plots of residual variation variances of the PLS regression showed that two factors were enough for the prediction for the density and crystallinity while four factors were required for the prediction of the melting point. Good straight-line fits could be obtained between the actual and predicted physical properties. Table III summarizes the correlation coefficient (R) and root-mean-square error of crossvalidation (RMSECV). The prediction of the melting point yields slightly worse results compared to the other parameters.

Figure 6 depicts a PLS loadings plot of factor 1 for the model shown in Figure 5(A). The corresponding plots for the models shown in Figure 5(B) and (C) are almost identical to the plot shown in Figure 6. The

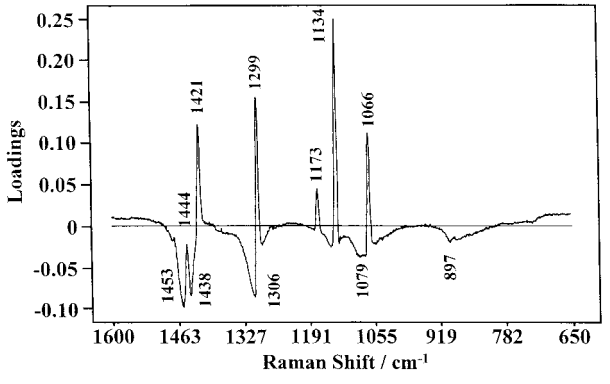

Figure 6 Loadings plot of factor 1 for the PLS-1 model shown in Figure 5 (A).

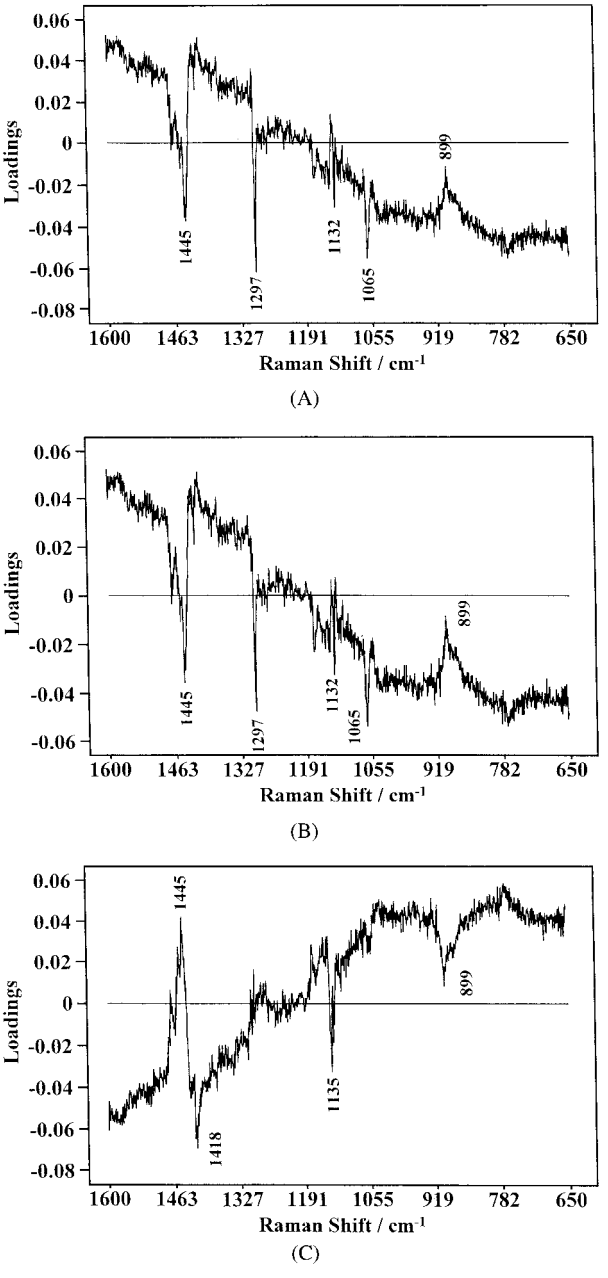

Figure 7 (A–C) PLS loadings plots of factor 2 for the models shown in Figure 5 (A), (B), and (C), respectively.

loadings plot in Figure 6 is very close to the PCA loadings plot in Figure 4(A). This result is consistent with our conclusion that factor 1 of the PCA score plot in Figure 3 reflects the density or crystallinity. Figure 7(A), (B), and (C) displays the PLS loadings plots of factor 2 for the models shown in Figure 5(A), (B), and (C), respectively. Of particular note in Figure 7(A), (B), and (C) is that the plots for the prediction of density and crystallinity are very similar but they are largely different from the loadings plot for the prediction of the melting point. The bands at 1445, 1297, 1132, and 1065 cm^{-1}, which are characteristic of the crystal structure, appear downward in the plots shown in Figure 7(A) and (B), but in the plot in Figure 7(C) the band at 1445 cm^{-1} appears upward while those at 1418 and 1135 cm^{-1} appear downward.

CONCLUSION

By use of PCA the Raman spectra of HDPE, LDPE, and LLDPE have been clearly discriminated. Factor 1 of the PCA reflects the crystallinity and density of PEs. Furthermore, we have been able to develop good PLS calibration models that predict the density, crystallinity, and melting point of PEs.

The loadings plots for the PCA score plot in Figure 3 and for the PLS models predicting the physical properties have shown resolution enhancement of the Raman bands of the different PEs. For example, the loadings plot of factor 1 for the PCA score plot has revealed the existence of bands at 1453 and 1438 cm^{-1}. The PLS loadings plot of factor 2 for the model predicting the melting point differs largely from those for the models predicting the density and crystallinity. Based on these investigations a fast, nondestructive and reliable quality control system for the different polyethylene types can be established.

REFERENCES

1. Siesler, H. W.; Holland-Moritz, K. Infrared and Raman Spectroscopy of Polymers, Practical Spectroscopy Series Vol. 4; Marcel Dekker: New York, 1980.
2. Hummel, D. O., Ed. Polymer Spectroscopy; Verlag Chemie: Weinheim, 1974.
3. Klopffer, W. Introduction to Polymer Spectroscopy; Springer-Verlag: New York, 1984.
4. Batchelder, D. N.; Chang, C.; Pitt, G. D. Adv Mater 1991, 3, 566.
5. Fawcett, A. H., Ed. Polymer Spectroscopy; John Wiley & Sons, Chichester, 1996, Chapts 7 and 8.
6. Everall, N.; Tayler, P.; Chalmers, J.; Ferweerda, R.; van der Maas, J. Polymer 1994, 35, 3184.
7. Zerbi, G.; Del Zoppo, M. In Modern Polymer Spectroscopy; Zerbi, G., Ed.; Wiley-VCH: Weinheim, 1999, p. 87.
8. Pelletier, M. J., Ed. Analytical Applications of Raman Spectroscopy; Blakwell Science: Oxford, UK, 1999.
9. Noda, I. Appl Spectrosc 1993, 47, 1329.
10. Noda, I.; Dowrey, A. E.; Marcott, C.; Story, G. M.; Ozaki, Y. Appl Spectrosc 2000, 54, 236A.
11. Ozaki, Y.; Noda, I., Eds. Two-Dimensional Correlation Spectroscopy; American Institute of Physics: New York, 2000.
12. Martens, H.; Naes, T. Multivariate Calibration; John Wiley & Sons: New York, 1989.
13. Vandenginste, B. G. M.; Massart, D. L.; Buydens, L. M. C.; de Jong, S.; Lewi, P. J.; Smeyers-Verbecke, J. Handbook of Chemometrics and Qualimetrics; Elsevier: Amsterdam, 1998.
14. Kramer, R. Chemometric Techniques for Quantitative Analysis; Marcel Dekker: New York, 1998.
15. Leugers, M. A.; Lipp, E. D. In Spectroscopy in Process Analysis; Chalmers, J. M., Ed.; Sheffield Academic Press: Sheffield, 2000, p. 139.
16. Lipp, E. D.; Leugers, M. A., in ref. 8, p. 106.
17. Everall, N. in ref. 8, p. 127.
18. Cooper, F. B. in ref. 8, p. 193.
19. Adar, F.; Geiger, R.; Noonan, J. Appl Spectrosc Revs 1997, 32, 45.
20. Everall, N. J. in An Introduction to Laser Spectroscopy; Andrews, D. L.; Demidov, A. A., Eds.; Plenum Press: New York, 1995, p. 115.
21. Chalmers, J. M.; Dent, G. Industrial Analysis with Vibrational Spectroscopy; Royal Society of Chemistry: Cambridge, UK, 1997, p. 241.
22. Gerrard, D. L. Anal Chem 1994, 66, 547R.
23. Vickers, T. J.; Mann, C. K. Analytical Raman Spectroscopy; Grasselli, J. G.; Bulkin, B. J., Eds., Wiley Interscience: New York, 1991, p. 107.
24. Shimoyama, M.; Maeda, H.; Matsukawa, K.; Inoue, H.; Ninomiya, T.; Ozaki, Y. Vib Spectrosc 1997, 14, 253.
25. Sano, K.; Shimoyama, M.; Ohgane, M.; Higashiyama, H.; Watari, M.; Tomo, M.; Ninomiya, T.; Ozaki, Y. Appl Spectrosc 1999, 53, 551.
26. Furukawa, T.; Watari, M.; Siesler, H. W.; Ozaki, Y., submitted for publication.
27. Bandermann, F.; Tausendfreund, I.; Šašic, S.; Ozaki, Y.; Kleimann, M.; Westerhuis, J. A.; Siesler, H. W. Macromol Rapid Commun 2001, 22, 690.
28. Šašic, S.; Amari, T.; Siesler, H. W.; Ozaki, Y. Appl Spectrosc, to appear.
29. Jiang, J.-H.; Ozaki, Y.; Kleimann, M.; Siesler, H. W., submitted for publication.
30. Bentley, P. A.; Hendra, P. J. Spectrochim Acta Part A 1995, 51, 2125.
31. Boerio, F. J.; Koenig, J. L. J Chem Phys 1970, 52, 3425.
32. Glotin, M.; Domszy, R.; Mandelkern, L. J Polym Sci Polym Phys Ed 1983, 21, 285.
33. Tarazona, A.; Koglin, E.; Coussens, B. B.; Meier, R. J. Vib Spectrosc 1997, 14, 159.
34. Strobl, G. R.; Hagedorn, W. J Polym Sci Polym Phys Ed 1978, 16, 1181.